

PpIT domain proteins – ubiquitous potential prokaryotic phospholipid translocases

Janna N. Hauser^{1,2,3}, Arnaud Kengmo Tchoupa^{1,2,3}, Susanne Zabel⁴, Kay Nieselt^{3,4}, Christoph M. Ernst^{1,5},
Christoph J. Slavetinsky^{1,2,3,6#}, Andreas Peschel^{1,2,3#}

1. Interfaculty Institute of Microbiology and Infection Medicine Tübingen, Infection Biology Section,
University of Tübingen, Germany.

2. German Center for Infection Research (DZIF), partner site Tübingen, Germany.

3. Cluster of Excellence EXC2124 Controlling Microbes to Fight Infection, University of Tübingen,
Germany

4. Institute for Bioinformatics and Medical Informatics, University of Tübingen, Germany

5. Current address: Department of Molecular Biology, Massachusetts General Hospital, Harvard
Medical School, Boston, MA, USA

6. Pediatric Surgery and Urology, University Children's Hospital Tübingen, University of Tübingen,
Germany.

Equally contributing corresponding authors. Correspondence to: Christoph J. Slavetinsky and
Andreas Peschel, Interfaculty Institute of Microbiology and Infection Medicine, Infection Biology
Section, University of Tübingen, Auf der Morgenstelle 28, 72076 Tübingen, Germany.

1 **Abstract**

2 Flippase proteins exchanging phospholipids between the cytoplasmic membrane leaflets have been
3 identified in Eukaryotes but remained largely unknown in Prokaryotes. Only MprF proteins that
4 synthesize aminoacyl phospholipids in some bacteria have been found to contain a domain that
5 translocates the produced lipids. We show here that this domain, which we named 'prokaryotic
6 phospholipid translocator' (PpIT), is widespread in Bacteria and Archaea, encoded as a separate
7 protein or fused to different types of enzymes. We also demonstrate that the *Escherichia coli* PpIT
8 protein interacts with many phospholipid-synthetic enzymes and deletion of *ppIT* impaired bacterial
9 growth, which supports its potential role in membrane lipid metabolism. PpIT domain proteins may
10 be general prokaryotic lipid flippases with critical roles in cellular homeostasis.

11

12 **Introduction**

13 Most of the basic processes and enzyme systems involved in growth and maintenance of prokaryotic
14 cells have been explored in the past. Major mechanisms of membrane lipid synthesis and turnover
15 have also been described thoroughly [1, 2]. However, 'flippase' proteins that facilitate the
16 translocation of phospholipids from the inner leaflet, the site of synthesis, to the outer leaflet of the
17 cytoplasmic membrane, have remained largely unknown. We speculated that such flippases might be
18 among the conserved membrane proteins of unknown function found in many prokaryotic taxa.
19 Phospholipid flippases may not be essential for cell viability, which might explain why they have not
20 been identified in previous screening approaches for prokaryotic proteins with crucial function for
21 cellular integrity. Flippases have been characterized in eukaryotic cells [3] but the responsible proteins
22 do not seem to have obvious homologs in prokaryotes.

23 Flippase reactions are particularly difficult to study because the flipping process is fast and hard to
24 monitor as the lipids remain in place and adapt only their orientation. Nevertheless, a prototype
25 flippase has been identified in prokaryotic MprF proteins that synthesize and then translocate
26 aminoacyl phosphatidylglycerol (Aa-PG) lipids such as lysyl-phosphatidylglycerol (Lys-PG) or alanyl-

27 phosphatidylglycerol (Ala-PG) [4, 5]. Those lipids reduce the negative net charge at the outer surface
28 of cytoplasmic membranes, thereby diminishing the binding of cationic antimicrobial molecules such
29 as bacterial bacteriocin and host defensin peptides [6]. To achieve protection against such molecules,
30 it is critical for microorganisms to efficiently translocate Lys-PG or Ala-PG, once these lipids have been
31 formed by the MprF synthase domain at the inner surface of the cytoplasmic membrane. The synthase
32 domain cooperates with the flippase domain in a dynamic fashion to deliver the lipid products to the
33 translocation channel [7]. The two domains function together even if expressed as separate proteins
34 [8]. The flippase domain of MprF consists of eight transmembrane sections [8] and contains a motif
35 that is accessible from both sides of the cytoplasmic membrane [9]. It has been proposed that this part
36 moves during the lipid translocation process or that it is in the center between two larger cavities that
37 form the lipid translocation channel [9]. The structure of the *Rhizobium tropici* MprF protein with
38 bound Lys-PG molecules captured in the process of translocation has recently been elucidated by cryo-
39 electron microscopy [7]. It gives rise to a mechanistic model that proposes a process with Lys-PG
40 entering an inner protein cavity, which transiently opens a gate to an outer cavity, from which Lys-PG
41 is subsequently released to the outer membrane leaflet [7]. The extent to which the flippase domain
42 found in MprF proteins is present in Bacteria and Archaea, and if it may play a more general role in
43 phospholipid translocation, has remained unknown.

44 The flippase domain of MprF proteins exhibits a conserved architecture with low sequence identity. It
45 is referred to as cl04219, pfam03706, or UPF0104 in the NCBI Conserved Domain Database (CDD) [10]
46 and as IPR022791 in the InterPro protein signatures database [11]. We show here that proteins
47 consisting of this domain alone or in combination with various enzymatic domains are found in almost
48 all of the major groups of Bacteria and Archaea, probably to accomplish the translocation of membrane
49 lipids. The corresponding *Escherichia coli* protein interacts with most of the phospholipid-biosynthetic
50 enzymes and it is encoded in the vicinity of a cardiolipin (CL) synthase. Its inactivation is not lethal but
51 affects the fitness of *E. coli*. We suggest naming the corresponding flippase domain ‘prokaryotic

52 phospholipid translocator' (PpIT), which is likely to fulfill a general membrane homeostatic function in
53 prokaryotes.

54

55 **Results**

56 **1. PpIT domain proteins are widespread in most groups of prokaryotes.** MprF-related proteins are
57 found in many different bacterial taxa [12]. Notably, we found that the two functional domains of MprF
58 occur in different combinations. The Lys-PG synthase domain, for instance, occurs sometimes without
59 the Lys-PG flippase domain [12]. On the other hand, the flippase domain is often encoded without a
60 Lys-PG synthase or in combination with other enzymatic domains. Systematic evaluation of microbial
61 genomes for the presence of this domain, referred to as PpIT (cl04219), revealed an almost universal
62 occurrence in most phyla of Bacteria (Fig. 1A) and in several Classes of Archaea (Fig. 1B). Indeed, blastp
63 searches uncovered that the PpIT domain is even found in bacterial species, which do not produce Aa-
64 PGs, such as *E. coli* and many other Enterobacteriaceae [13, 14]. Thus, PpIT may have a broader role in
65 prokaryotes than previously thought. It should be noted that most prokaryotes with a *ppiT* homolog
66 encode only one protein with a PpIT domain in their genome (Fig. S1).

67 PpIT occurs as a separate protein in many different bacterial phyla including Proteobacteria,
68 Actinobacteria, Firmicutes, Bacteroidetes, Planctomycetes, and Thermotogae as well as archaeal phyla
69 including Euryarchaeota and Crenarchaeota. Moreover, PpIT is found connected to other types of
70 proteins in addition to Lys-PG or Ala-PG synthases (Fig. 2). The Conserved Domain Architecture
71 Retrieval Tool [15] lists 148 different architectures of PpIT domain-containing proteins. The most
72 prevalent architectures include combinations with Aa-PG synthase domain (cl41273) of MprF proteins,
73 glycosyl transferase domains (family A, cl11394; or family B, cl10013), or protein kinase domains
74 (cl21453) (Fig. 2). MprF proteins were most often found in genomes of Cyanobacteria, Actinobacteria,
75 Firmicutes, and Proteobacteria. A C-terminal or N-terminal family-B glycosyltransferase domain was
76 found attached to PpIT proteins from Actinobacteria, Nitrospirae, and Chloroflexi or Acidobacteria,

77 respectively, while a family-A glycosyltransferase domain was found at the N-terminus of PpIT in
78 Archaea of the Euryarchaeota phylum. Several Actinobacteria encode a protein kinase domain, N-
79 terminally fused to PpIT. Further, less frequently occurring combinations were found with enzymatic
80 domains such as dehalogenase-like hydrolases (cl21460), O-antigen ligases (cl04850), S-
81 adenosylmethionine-dependent methyltransferase (cl17173), or phosphotransferases (cl37506), to
82 name a few (Fig. 2). These findings suggest that PpIT-containing proteins may have multiple roles,
83 presumably in the synthesis, modification, and translocation of different types of membrane lipids or
84 in membrane-linked signal transduction processes. In several bacterial and archaeal taxa, only a
85 minority of the genera appear to encode PpIT proteins in their genomes (Fig. 1) suggesting that PpIT
86 proteins may be important only in certain habitats or that some bacteria may use other transport
87 systems, that could translocate phospholipids along with other types of cargo molecules.

88 **2. The *E. coli* PpIT is encoded together and interacts with lipid-synthetic enzymes.** In order to study
89 potential functions of PpIT proteins not linked to other protein domains, we focused on the *E. coli*
90 homolog, a protein of unknown function with the generic name YbhN, we suggest to rename PpIT.
91 *ppiT* is not essential in *E. coli*, mutations in this gene are included in the Keio collection, a transposon
92 mutant library [16], albeit without a reported phenotype. *ppiT* is encoded in an operon together with
93 the CL synthase gene *clsB* in *E. coli* and other Enterobacteriaceae including the genera *Shigella*,
94 *Klebsiella* and *Pantoea* (Fig. 3A), which is in agreement with the role of PpIT in lipid synthesis and
95 translocation.

96 Phospholipid-biosynthetic proteins have been found to form large multicomponent complexes in
97 bacteria such as *S. aureus* [17, 18]. To analyze a role of PpIT in such complexes, its potential interaction
98 with several phospholipid-biosynthetic proteins was studied in the bacterial two-hybrid system [8, 19,
99 20]. The genes to be analyzed were cloned in *E. coli* expression plasmids, resulting in C- and N-terminal
100 fusions of potential interaction partners or PpIT with the complementary adenylate cyclase fragment
101 T18 or T25, respectively. Interaction of T18 with T25 results in the production of cAMP, leading to
102 expression of β-galactosidase, which was quantified. *E. coli* does not produce aminoacyl phospholipids

103 but, in addition to phosphatidylglycerol (PG) and CL, phosphatidylserine (PS) and
104 phosphatidylethanolamine (PE) [2]. PpIT was found to interact with the proteins PgpA, PgpB, and PgpC,
105 involved in PG synthesis and with the CL synthase ClsB, encoded in the same operon as PpIT (Fig. 3A,
106 B, C). Hence, PpIT interacts with the majority of PG and CL biosynthetic enzymes in *E. coli* (Fig. 3C),
107 which supports a role of PpIT in phospholipid metabolism.

108 **3. PpIT affects *E. coli* fitness.** Although *ppIT* is not essential in *E. coli*, its ubiquitous presence in most
109 of the prokaryotic taxa suggests an important role in basic cellular functions. *ppIT* was deleted in the
110 uropathogenic *E. coli* (UPEC) strain CFT073. The mutant had the same phospholipid pattern as the wild
111 type (WT) indicating that PpIT has no obvious impact on the overall lipid composition (Fig. 4A, B). The
112 *ppIT* mutant exhibited a growth defect compared with the WT in the late logarithmic phase and it did
113 not reach the cell density of WT cultures (Fig. 5). This phenotype was pronounced at 37°C (Fig. 5A) but
114 not observed at 42°C (Fig. 5B), which supports a role of PpIT in optimal membrane function, a process
115 that depends on temperature. When co-cultivated over several days, the WT grew better than the *ppIT*
116 mutant (Fig. 5C, D), demonstrating a competitive fitness benefit conferred by PpIT.

117

118 **Discussion**

119 Phospholipids are synthesized at the inner leaflet of the cytoplasmic membrane but they need to be
120 translocated to the outer leaflet to form a stable bilayer [1]. Phospholipids can flip spontaneously but
121 this process is rather inefficient [21]. Appropriate membrane homeostasis therefore depends on
122 dedicated flippases that translocate lipids. While such transporters are known for eukaryotic cells, their
123 presence and nature in prokaryotes has remained largely unclear. ABC transporters translocating the
124 lipid-bound precursors of peptidoglycan or teichoic acids have been identified [22, 23]. However, these
125 molecules are usually highly specific and are unlikely to have a major impact on phospholipid
126 translocation. Nevertheless, the lipid-A translocating ABC transporter MsbA of *E. coli* has also a minor
127 affinity for phospholipids [23]. The only dedicated bacterial phospholipid flippase described to date is

128 the integral-membrane domain of MprF proteins, which connects the synthesis of aminoacyl
129 phospholipids with their translocation [4, 5]. We show here that the flippase domain of MprF, named
130 the PpIT domain, can be found as a separate protein or combined in modular proteins with other
131 domains of diverse function, which supports a general role of PpIT in bacterial and archaeal cells.

132 The PpIT protein modulates the fitness of *E. coli*. The observed effects were moderate, which may be
133 based on the fact that the lipid A flippase MsbA has also some basic phospholipid translocation
134 capacity [23] and may compensate for the lack of PpIT to some degree. *msbA* is essential though [16,
135 24], which precludes its simultaneous inactivation with *ppIT*. The residual capacity of MsbA cell wall
136 precursor flippases to translocate phospholipids may also explain why several bacterial species do not
137 seem to encode obvious PpIT orthologs. Membrane function is strongly affected by temperature,
138 which may explain the temperature-dependent impact of PpIT in *E. coli*. It should be noted though that
139 PpIT domain proteins are also found in thermophilic microorganisms such as Thermotogae and
140 archaeal extremophiles, suggesting that the translocation of certain lipids may require dedicated
141 flippases even at high temperatures. The frequent combination of PpIT with other enzymatic protein
142 domains also suggests that certain modified lipids, potentially those with bulkier head groups, may be
143 particularly dependent on cognate translocation machineries. Lipid translocation is a very dynamic
144 process, which is difficult to monitor directly. Therefore, evidence for the flippase function of PpIT
145 proteins remains in part indirect. However, the fact that PpIT interacts directly with most of the
146 phospholipid-biosynthetic proteins of *E. coli* underscores its central role in membrane homeostasis.
147 Likewise, MprF proteins have been found to interact with larger phospholipid-biosynthetic protein
148 complexes in *S. aureus* [17, 18].

149 It remains unclear how wide or narrow the substrate specificities of PpIT domain proteins may be.
150 Since *E. coli* does not produce aminoacyl phospholipids, PpIT may translocate some or all of the *E. coli*
151 phospholipids PG, CL, PS, and PE. These molecules differ in the net charge of their head groups, which
152 has been found to be a major determinant for substrate recognition by the PpIT domain of the *R. tropici*
153 MprF [7]. Although the PpIT domain of the *S. aureus* MprF is linked to synthesis of the cationic

154 phospholipid Lys-PG, MprF has been found to also translocate the zwitterionic phospholipid Ala-PG
155 [25], indicating that PpIT proteins may have broader substrate specificities. It should be noted that
156 most prokaryotic genomes with a PpIT homolog contain only one PpIT protein and only a minority
157 encodes two (19.89%) or more (1.60%) of them, suggesting that one flippase may usually be sufficient
158 for most of the membrane-forming phospholipids. Archaea have different phospholipids compared to
159 bacterial ones, with monolayer-membrane forming isoprenoid lipids [27]. The broad presence of PpIT
160 proteins in Archaea suggest that these proteins may also be able to flip such lipids, which are much
161 bulkier than bacterial phospholipids and contain two head groups, one at each end. It remains unclear
162 if the PpIT domain may only facilitate the exchange of phospholipids between the inner and outer
163 leaflet of cytoplasmic membranes or if it can translocate phospholipids in an energy-dependent
164 fashion to generate asymmetric lipid patterns. Some of the transmembrane domains of MprF seem to
165 be related to the proton-motif force-dependent major facilitator protein superfamily [28] and some
166 studies found Lys-PG to be unevenly distributed between the two membrane leaflets [4], suggesting
167 that PpIT may use energy to translocate its substrate lipids.

168 Membrane homeostasis is an important fitness factor for all kinds of organisms. PpIT proteins may
169 therefore become attractive targets for future anti-fitness drugs to combat major human pathogens.
170 In support of such a strategy, monoclonal antibodies directed against extracellular portions of the PpIT
171 domain of the *S. aureus* MprF have recently been shown by inhibiting the Lys-PG exposure at the outer
172 leaflet of the membrane and therefore sensitize *S. aureus* to cationic antibiotics [9].

173

174 Materials and Methods

175 **Occurrence and architecture of PpIT in bacterial and archaeal taxa.** In order to determine the
176 distribution of PpIT across the taxonomy a blastp search within NCBI's non-redundant protein database
177 [29] was performed using the PpIT/YbhN protein sequence of *E. coli* (old: NP_752801.1; new:
178 WP_000045478.1) as a query and an E-value cutoff of 0.05. Blast hits originating from the

179 superkingdoms Bacteria and Archaea were investigated separately. For each, the subtree of the NCBI
180 taxonomy rooted at the respective superkingdom was thinned out for those taxa that possess a PpIT
181 homolog. The BLAST search and subsequent taxonomic visualization was performed with BLASTphylo
182 [<https://github.com/Integrative-Transcriptomics/BLASTphylo>]. We used NCBI's Conserved Domain
183 Architecture Retrieval Tool (CDART) [15] to identify different domain architectures that include a PpIT
184 domain. We used MicrobesOnline[30] to identify *ppIT*'s operon structure in other Enterobacteriaceae.

185 **Bacterial strains, mutagenesis, and maintenance.** *E. coli* UPEC strain CFT073 (DSM103538) (Tab. S1)
186 was used for *ppIT* mutagenesis and analysis [31]. *ppIT* was deleted in the chromosome of CFT073 as
187 described previously [32]. Briefly, *E. coli* CFT073 was transformed with helper plasmid pKD46 encoding
188 the Lambda-Red recombinase (Tab. S2) and incubated at 30°C on LB agar supplemented with
189 ampicillin. The kanamycin resistance cassette with chromosomal DNA regions flanking *ppIT* was
190 amplified by PCR with primers ppIT_KO_5 and ppIT_KO_6 (Tab. S3) using pKD13 as template (Tab. S2).
191 After arabinose-induced Lambda Red expression in *E. coli* CFT073 containing the helper plasmid, the
192 PCR fragment was transferred by electroporation and cells were plated on kanamycin-containing LB
193 agar for primary selection. After verification of the chromosomal *ppIT* deletion by PCR (Tab. S3) and
194 sequencing, mutants were streaked to single colonies on LB agar without antibiotics at 37°C twice for
195 curing of the temperature-sensitive helper plasmid. The loss of the helper plasmid pKD46 was
196 confirmed by PCR (Tab. S3). The *ppIT* deletion mutant was complemented by a *ppIT* gene amplified
197 from *E. coli* K12 and cloned in the *E. coli*/*S. aureus* shuttle vector pRB474 [33] (Tab. S2). All bacterial
198 strains were grown in LB medium (Carl Roth) with appropriate antibiotics unless otherwise noted (Tab.
199 S1).

200 **Bacterial two-hybrid assay.** To identify potential interaction partners of PpIT, the commercially
201 available bacterial two-hybrid kit (BATCH kit, Euromedex) was used [8, 19, 20] and the proteins to be
202 studied were cloned as described previously [8]. The *ppIT* gene was cloned in the high-copy number
203 plasmid pUT18C, the potential interaction partners in the low copy-number plasmid pKT25 leading to
204 C-terminal or N-terminal fusion with the adenylate cyclase fragments T25 or T18 of *Bordetella*

205 *pertussis*, respectively (Tab. S2). The constructs were used to co-transform chemically competent *E.*
206 *coli* BTH101. The resulting transformants were tested in a 96-well format for β -galactosidase activity,
207 to quantify the protein-protein interaction as described previously [8] with slight modifications. Briefly,
208 bacterial cells were grown at 30°C overnight in LB, supplemented with 0.5 mM isopropyl- β -D-
209 thiogalactopyranoside (IPTG), 25 μ g/ml kanamycin and 100 μ g/ml ampicillin. 100 μ l of the overnight
210 cultures were used to measure the optical density at 600 nm (OD₆₀₀) in a 96-well microtiter plate (F-
211 bottom, Falcon), another 100 μ l were transferred into a deep 96-well plate (U-bottom, Sarstedt) and
212 mixed with 1 ml buffer Z (60 mM Na₂HPO₄, 40 mM NaH₂PO₄, 10 mM KCl, 1 mM MgSO₄, 50 mM β -
213 mercaptoethanol). To lyse the cells, 40 μ l sodium dodecyl sulfate (0.1%) and 80 μ l chloroform were
214 added and mixed vigorously. After incubation at room temperature to allow phase separation, 100 μ l
215 of the aqueous phase were transferred into a 96-well microtiter plate (F-bottom, Falcon) and mixed
216 with 20 μ l o-nitrophenyl- β -D-galactopyranoside (4 mg/ml) to start the enzymatic reaction. The
217 reaction was measured continuously for 1 h in a CLARIOStar plate reader (BMG Labtech) at OD₄₂₀ and
218 OD₅₅₀. The β -galactosidase activity in Miller Units was calculated by the formula: 1000*((OD₄₂₀-
219 (1.75*OD₅₅₀))/(t*v*OD₆₀₀)), where t is reaction time in minutes and v the reaction volume in milliliter.

220 **Isolation of polar lipids.** Polar lipids were extracted from bacteria grown to exponential or stationary
221 phase using the Bligh-Dyer procedure [34]. Briefly, phospholipids were extracted by a mixture of
222 sodium acetate buffer (20mM, pH 4.8), chloroform, and methanol (1:1:1 [by volume]), vacuum dried,
223 and dissolved in chloroform-methanol (2:1 [by volume]). For detection of phospholipid patterns,
224 appropriate amounts of polar lipid extracts were spotted onto silica gel high-performance thin-layer
225 chromatography (HPTLC) plates (silica gel 60 F₂₅₄, Merck) using a Linomat 5 sample application unit
226 (CAMAG) and developed with chloroform:methanol:water (65:25:4 [by volume]) in an automatic
227 developing chamber ADC 2 (CAMAG). Phospholipids were selectively stained with molybdenum blue
228 spray reagent (1.3% in 4.2 M sulfuric acid, Sigma-Aldrich).

229 **Bacterial growth assay.** Temperature-dependent growth differences were analyzed in 96-well
230 microtiter plate format. To this end, overnight cultures grown in LB with appropriate antibiotics were

231 adjusted to OD₆₀₀ 0.05 in fresh LB and 100 µl of the cell suspensions were transferred to a 96-well
232 microtiter plate (F-bottom, Falcon) and growth was measured at OD₆₀₀ in 30 min intervals at either
233 37°C or 42°C in an Epoch2 plate reader (BioTek).

234 To investigate growth differences of WT and *ppi/T* mutant in cocultivation, overnight cultures were
235 adjusted to the same colony forming unit in fresh LB and used to inoculate a coculture, which was
236 incubated in a shaking incubator at either 37°C or 42°C. Cells were passaged every 24 h in fresh LB for
237 five days. To measure the numbers of live cells of the two competing strains, appropriate dilutions of
238 the suspensions were spotted on LB agar plates with or without kanamycin. After incubation of the
239 agar plates at appropriate temperatures, colonies were counted and ratios were calculated.

240 **Statistics.** Statistical analyses were performed with the Prism 8.4.2 package (GraphPad Software) and
241 Group differences were analyzed for significance with one-way or two-way ANOVA. A *P* value of ≤0.05
242 was considered statistically significant.

243

244 **Acknowledgments**

245 We thank Anne Berscheid for providing plasmids pKD13 and pKD46, Cordula Gekeler and Ulrike Redel
246 for technical support and Jennifer Müller for her contributions to the BLASTphylo project. This work
247 was financed by Grants from Deutsche Forschungsgemeinschaft (DFG) SFB766 (to A.P.) and TRR261,
248 project ID 398967434 (to K.N. and A.P), the German Center of Infection Research (DZIF) (to A.P. and
249 C.S.). C.S. was also supported by the intramural Experimental Medicine program of the Medical Faculty
250 at the University of Tübingen. The authors acknowledge project support (C.S.) and infrastructural
251 support (C.S., K.N., A.P.) by the DFG Cluster of Excellence EXC2124 CMFI, project ID 390838134.

252

References

1. Zhang YM, Rock CO. Membrane lipid homeostasis in bacteria. *Nat Rev Microbiol.* 2008;6(3):222-33. doi: 10.1038/nrmicro1839. PubMed PMID: 18264115.
2. Dowhan W, Bogdanov M, Eugene P. Kennedy's Legacy: Defining Bacterial Phospholipid Pathways and Function. *Front Mol Biosci.* 2021;8:666203. Epub 2021/04/13. doi: 10.3389/fmolb.2021.666203. PubMed PMID: 33842554; PubMed Central PMCID: PMCPMC8027125.
3. López-Marqués RL. Lipid flippases in polarized growth. *Curr Genet.* 2021;67(2):255-62. Epub 2021/01/04. doi: 10.1007/s00294-020-01145-0. PubMed PMID: 33388852.
4. Ernst CM, Staubitz P, Mishra NN, Yang SJ, Hornig G, Kalbacher H, et al. The bacterial defensin resistance protein MprF consists of separable domains for lipid lysinylation and antimicrobial peptide repulsion. *PLoS Pathog.* 2009;5(11):e1000660. Epub 2009/11/17. doi: 10.1371/journal.ppat.1000660. PubMed PMID: 19915718; PubMed Central PMCID: PMCPMC2774229.
5. Ernst CM, Peschel A. Broad-spectrum antimicrobial peptide resistance by MprF-mediated aminoacylation and flipping of phospholipids. *Mol Microbiol.* 2011;80(2):290-9. Epub 2011/02/11. doi: 10.1111/j.1365-2958.2011.07576.x. PubMed PMID: 21306448.
6. Peschel A, Jack RW, Otto M, Collins LV, Staubitz P, Nicholson G, et al. *Staphylococcus aureus* resistance to human defensins and evasion of neutrophil killing via the novel virulence factor MprF is based on modification of membrane lipids with l-lysine. *J Exp Med.* 2001;193(9):1067-76. Epub 2001/05/09. doi: 10.1084/jem.193.9.1067. PubMed PMID: 11342591; PubMed Central PMCID: PMCPMC2193429.
7. Song D, Jiao H, Liu Z. Phospholipid translocation captured in a bifunctional membrane protein MprF. *Nat Commun.* 2021;12(1):2927. Epub 2021/05/20. doi: 10.1038/s41467-021-23248-z. PubMed PMID: 34006869; PubMed Central PMCID: PMCPMC8131360.
8. Ernst CM, Kuhn S, Slavetinsky CJ, Krismer B, Heilbronner S, Gekeler C, et al. The lipid-modifying multiple peptide resistance factor is an oligomer consisting of distinct interacting synthase and flippase subunits. *mBio.* 2015;6(1). Epub 2015/01/30. doi: 10.1128/mBio.02340-14. PubMed PMID: 25626904; PubMed Central PMCID: PMCPMC4324311.
9. Slavetinsky CJ, Hauser JN, Gekeler C, Slavetinsky J, Geyer A, Kraus A, et al. Sensitizing *Staphylococcus aureus* to antibacterial agents by decoding and blocking the lipid flippase MprF. *eLife.* 2022;11. Epub 2022/01/20. doi: 10.7554/eLife.66376. PubMed PMID: 35044295.
10. Yang M, Derbyshire MK, Yamashita RA, Marchler-Bauer A. NCBI's Conserved Domain Database and Tools for Protein Domain Analysis. *Curr Protoc Bioinformatics.* 2020;69(1):e90. Epub 2019/12/19. doi: 10.1002/cpbi.90. PubMed PMID: 31851420; PubMed Central PMCID: PMCPMC7378889.
11. Blum M, Chang HY, Chuguransky S, Grego T, Kandasamy S, Mitchell A, et al. The InterPro protein families and domains database: 20 years on. *Nucleic Acids Res.* 2021;49(D1):D344-d54. Epub 2020/11/07. doi: 10.1093/nar/gkaa977. PubMed PMID: 33156333; PubMed Central PMCID: PMCPMC7778928.
12. Roy H, Ibba M. Broad range amino acid specificity of RNA-dependent lipid remodeling by multiple peptide resistance factors. *J Biol Chem.* 2009;284(43):29677-83. doi: 10.1074/jbc.M109.046367. PubMed PMID: 19734140; PubMed Central PMCID: PMCPMC2785599.
13. Cronan JE, Jr., Rock CO. Biosynthesis of Membrane Lipids. *EcoSal Plus.* 2008;3(1). Epub 2008/09/01. doi: 10.1128/ecosalplus.3.6.4. PubMed PMID: 26443744.
14. Furse S, Wienk H, Boelens R, de Kroon AI, Killian JA. *E. coli* MG1655 modulates its phospholipid composition through the cell cycle. *FEBS Lett.* 2015;589(19 Pt B):2726-30. Epub 2015/08/15. doi: 10.1016/j.febslet.2015.07.043. PubMed PMID: 26272829.
15. Geer LY, Domrachev M, Lipman DJ, Bryant SH. CDART: protein homology by domain architecture. *Genome Res.* 2002;12(10):1619-23. Epub 2002/10/09. doi: 10.1101/gr.278202. PubMed PMID: 12368255; PubMed Central PMCID: PMCPMC187533.
16. Baba T, Ara T, Hasegawa M, Takai Y, Okumura Y, Baba M, et al. Construction of *Escherichia coli* K-12 in-frame, single-gene knockout mutants: the Keio collection. *Mol Syst Biol.*

2006;2:2006.0008. Epub 2006/06/02. doi: 10.1038/msb4100050. PubMed PMID: 16738554; PubMed Central PMCID: PMCPMC1681482.

17. García-Lara J, Weihs F, Ma X, Walker L, Chaudhuri RR, Kasturiarachchi J, et al. Supramolecular structure in the membrane of *Staphylococcus aureus*. *Proc Natl Acad Sci U S A*. 2015;112(51):15725-30. Epub 2015/12/09. doi: 10.1073/pnas.1509557112. PubMed PMID: 26644587; PubMed Central PMCID: PMCPMC4697411.

18. Weihs F, Wacnik K, Turner RD, Culley S, Henriques R, Foster SJ. Heterogeneous localisation of membrane proteins in *Staphylococcus aureus*. *Sci Rep*. 2018;8(1):3657. Epub 2018/02/28. doi: 10.1038/s41598-018-21750-x. PubMed PMID: 29483609; PubMed Central PMCID: PMCPMC5826919.

19. Karimova G, Gauliard E, Davi M, Ouellette SP, Ladant D. Protein-Protein Interaction: Bacterial Two-Hybrid. *Methods Mol Biol*. 2017;1615:159-76. Epub 2017/07/02. doi: 10.1007/978-1-4939-7033-9_13. PubMed PMID: 28667611.

20. Griffith KL, Wolf RE, Jr. Measuring beta-galactosidase activity in bacteria: cell growth, permeabilization, and enzyme assays in 96-well arrays. *Biochem Biophys Res Commun*. 2002;290(1):397-402. Epub 2002/01/10. doi: 10.1006/bbrc.2001.6152. PubMed PMID: 11779182.

21. Kol MA, de Kroon AI, Killian JA, de Kruijff B. Transbilayer movement of phospholipids in biogenic membranes. *Biochemistry*. 2004;43(10):2673-81. Epub 2004/03/10. doi: 10.1021/bi036200f. PubMed PMID: 15005602.

22. Swoboda JG, Meredith TC, Campbell J, Brown S, Suzuki T, Bollenbach T, et al. Discovery of a small molecule that blocks wall teichoic acid biosynthesis in *Staphylococcus aureus*. *ACS Chem Biol*. 2009;4(10):875-83. Epub 2009/08/20. doi: 10.1021/cb900151k. PubMed PMID: 19689117; PubMed Central PMCID: PMCPMC2787957.

23. Eckford PD, Sharom FJ. The reconstituted *Escherichia coli* MsbA protein displays lipid flippase activity. *Biochem J*. 2010;429(1):195-203. Epub 2010/04/24. doi: 10.1042/bj20100144. PubMed PMID: 20412049; PubMed Central PMCID: PMCPMC2888566.

24. Karow M, Georgopoulos C. The essential *Escherichia coli* msbA gene, a multicopy suppressor of null mutations in the htrB gene, is related to the universally conserved family of ATP-dependent translocators. *Mol Microbiol*. 1993;7(1):69-79. Epub 1993/01/01. doi: 10.1111/j.1365-2958.1993.tb01098.x. PubMed PMID: 8094880.

25. Slavetinsky CJ, Peschel A, Ernst CM. Alanyl-phosphatidylglycerol and lysyl-phosphatidylglycerol are translocated by the same MprF flippases and have similar capacities to protect against the antibiotic daptomycin in *Staphylococcus aureus*. *Antimicrob Agents Chemother*. 2012;56(7):3492-7. Epub 2012/04/12. doi: 10.1128/aac.00370-12. PubMed PMID: 22491694; PubMed Central PMCID: PMCPMC3393434.

26. Ernst CM, Slavetinsky CJ, Kuhn S, Hauser JN, Nega M, Mishra NN, et al. Gain-of-Function Mutations in the Phospholipid Flippase MprF Confer Specific Daptomycin Resistance. *MBio*. 2018;9(6). Epub 2018/12/20. doi: 10.1128/mBio.01659-18. PubMed PMID: 30563904; PubMed Central PMCID: PMCPMC6299216.

27. Caforio A, Driessen AJM. Archaeal phospholipids: Structural properties and biosynthesis. *Biochim Biophys Acta Mol Cell Biol Lipids*. 2017;1862(11):1325-39. Epub 2016/12/23. doi: 10.1016/j.bbalip.2016.12.006. PubMed PMID: 28007654.

28. Wang SC, Davejan P, Hendargo KJ, Javadi-Razaz I, Chou A, Yee DC, et al. Expansion of the Major Facilitator Superfamily (MFS) to include novel transporters as well as transmembrane-acting enzymes. *Biochim Biophys Acta Biomembr*. 2020;1862(9):183277. Epub 2020/03/25. doi: 10.1016/j.bbamem.2020.183277. PubMed PMID: 32205149; PubMed Central PMCID: PMCPMC7939043.

29. O'Leary NA, Wright MW, Brister JR, Ciufo S, Haddad D, McVeigh R, et al. Reference sequence (RefSeq) database at NCBI: current status, taxonomic expansion, and functional annotation. *Nucleic Acids Res*. 2016;44(D1):D733-45. Epub 2015/11/11. doi: 10.1093/nar/gkv1189. PubMed PMID: 26553804; PubMed Central PMCID: PMCPMC4702849.

30. Dehal PS, Joachimiak MP, Price MN, Bates JT, Baumohl JK, Chivian D, et al. MicrobesOnline: an integrated portal for comparative and functional genomics. *Nucleic Acids Res*. 2010;38(Database

issue):D396-400. Epub 2009/11/13. doi: 10.1093/nar/gkp919. PubMed PMID: 19906701; PubMed Central PMCID: PMCPMC2808868.

31. Welch RA, Burland V, Plunkett G, 3rd, Redford P, Roesch P, Rasko D, et al. Extensive mosaic structure revealed by the complete genome sequence of uropathogenic Escherichia coli. *Proc Natl Acad Sci U S A*. 2002;99(26):17020-4. Epub 2002/12/10. doi: 10.1073/pnas.252529799. PubMed PMID: 12471157; PubMed Central PMCID: PMCPMC139262.

32. Datsenko KA, Wanner BL. One-step inactivation of chromosomal genes in Escherichia coli K-12 using PCR products. *Proc Natl Acad Sci U S A*. 2000;97(12):6640-5. Epub 2000/06/01. doi: 10.1073/pnas.120163297. PubMed PMID: 10829079; PubMed Central PMCID: PMCPMC18686.

33. Bruckner R. A series of shuttle vectors for *Bacillus subtilis* and *Escherichia coli*. *Gene*. 1992;122(1):187-92. PubMed PMID: 1452028.

34. Bligh EG, Dyer WJ. A rapid method of total lipid extraction and purification. *Can J Biochem Physiol*. 1959;37(8):911-7. Epub 1959/08/01. doi: 10.1139/o59-099. PubMed PMID: 13671378.

Figures

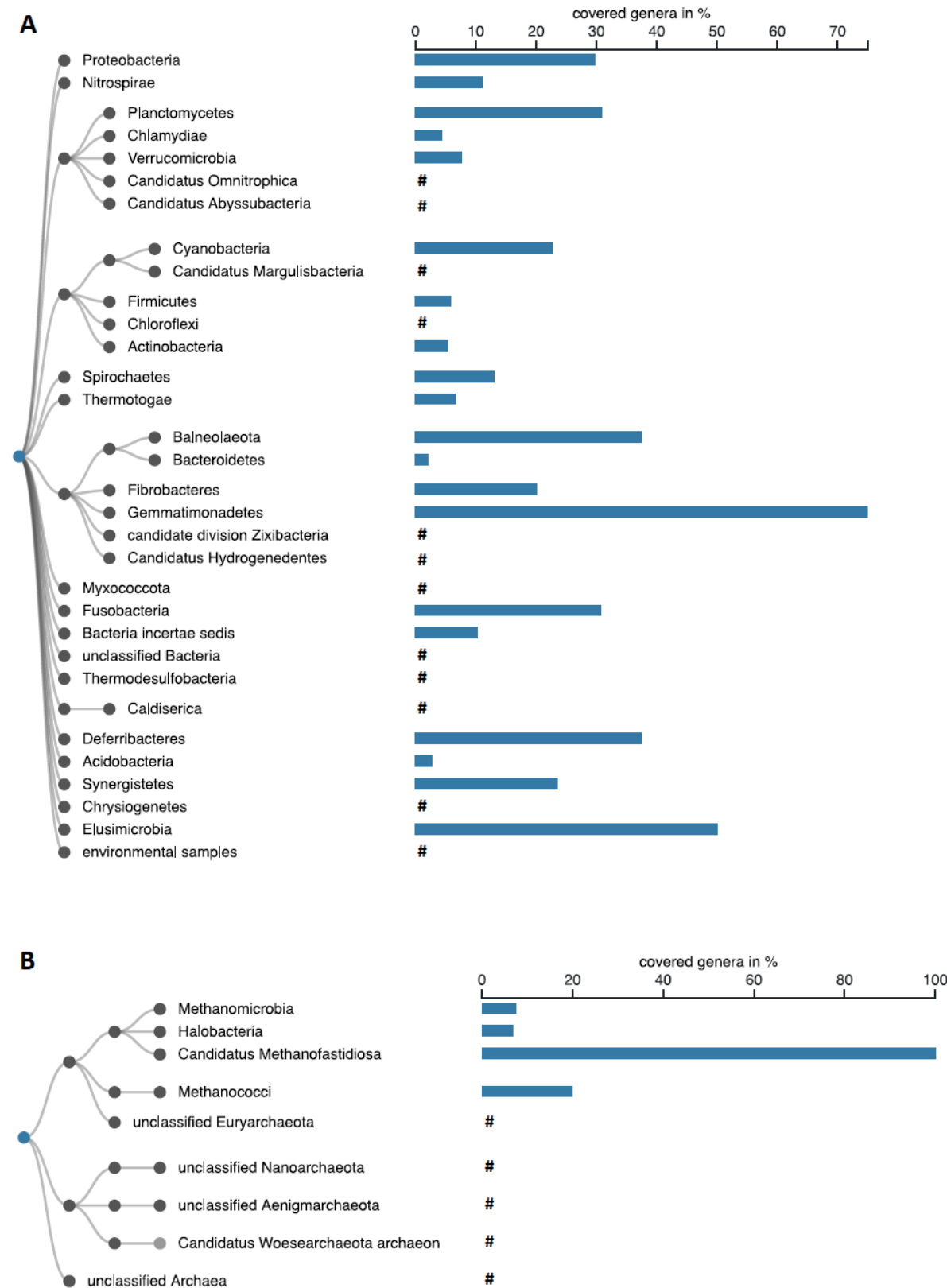


Figure 1: Distribution of the PpIT domain amongst taxa of the Bacteria (A) and Archaea (B) superkingdoms. The taxonomy was collapsed to the phylum rank. Dark grey leaf nodes indicate collapsed nodes. The bar chart indicates the fraction of genera of a particular Phylum (Bacteria) or

Class (Archaea) carrying a PpIT homolog within the subtree rooted at the respective taxon. #, taxa include *ppIT* genes but percentages of covered genera could not be calculated due to incomplete assignment of the genome on genus level.

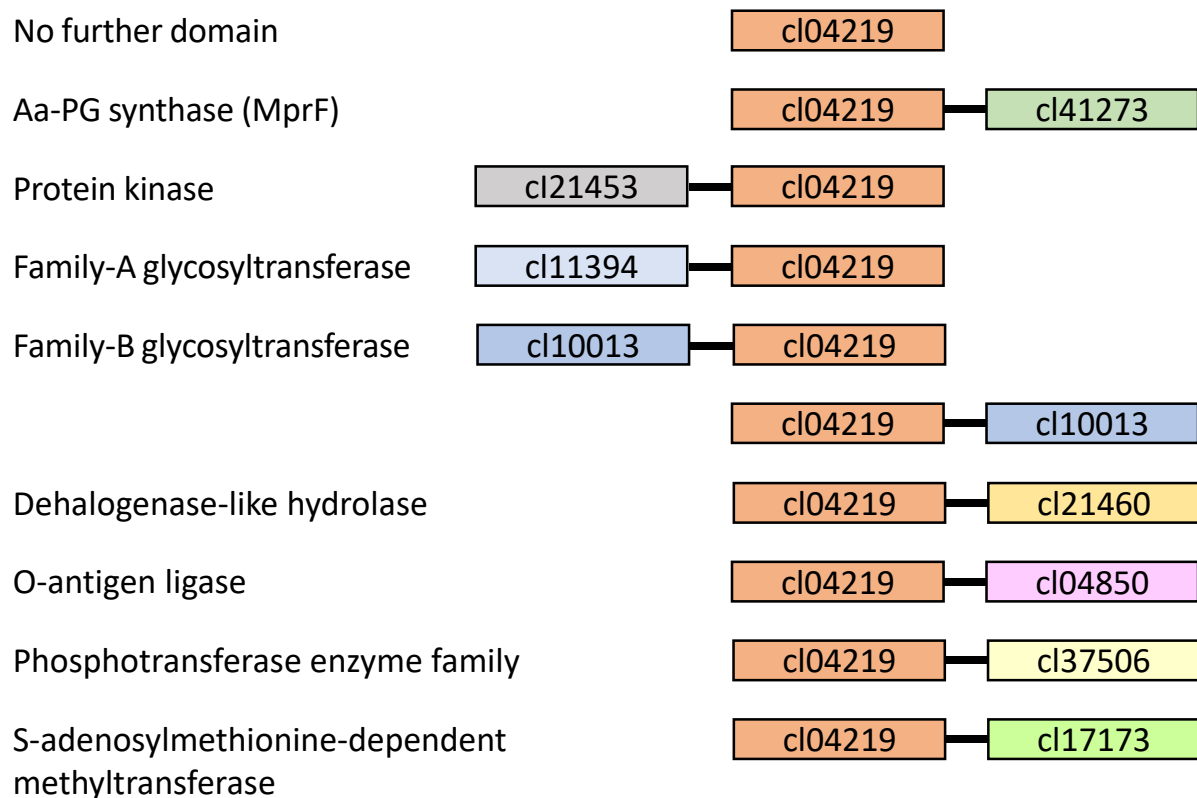


Figure 2: PpIT domain protein architectures. Combinations of the PpIT domain (cl04219) with other protein domains found in Bacteria and Archaea. The 10 most commonly occurring domain combinations are shown, as revealed by the Conserved Domain Architecture Retrieval Tool [15]. The domains are not drawn to scale.

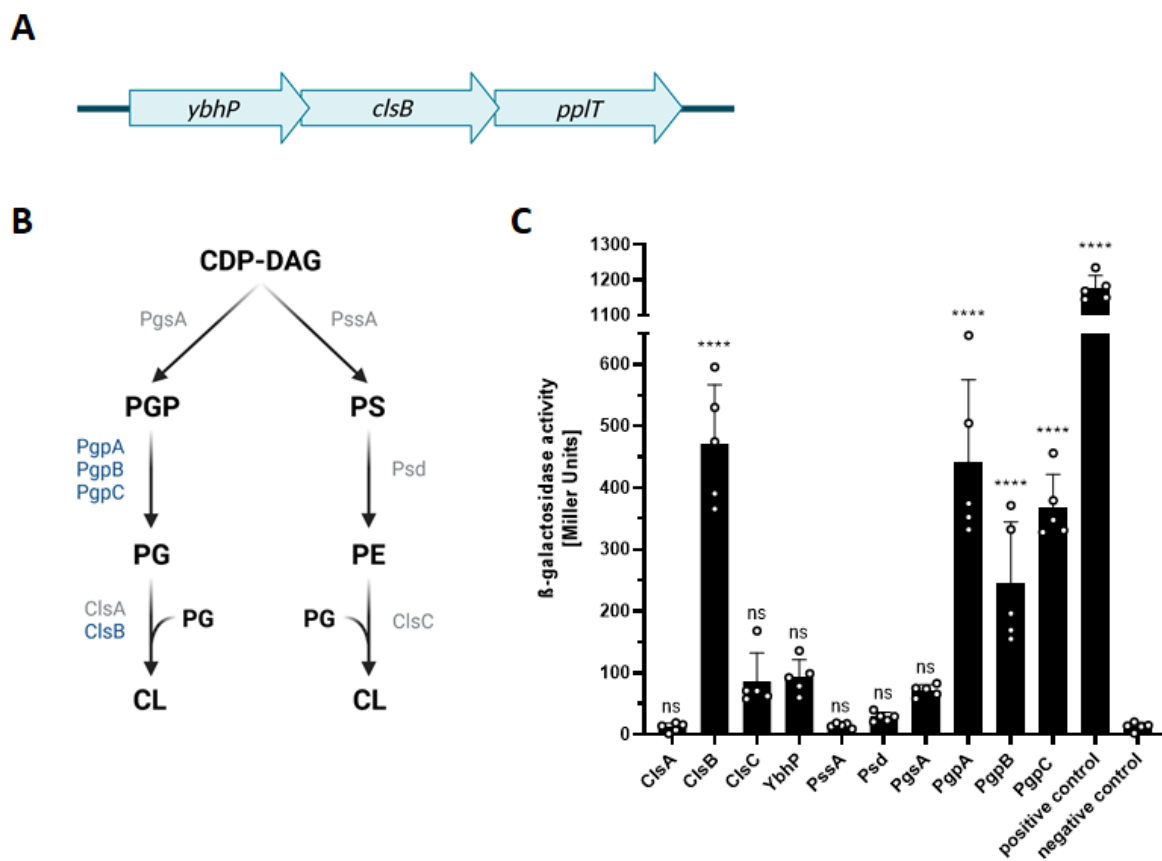
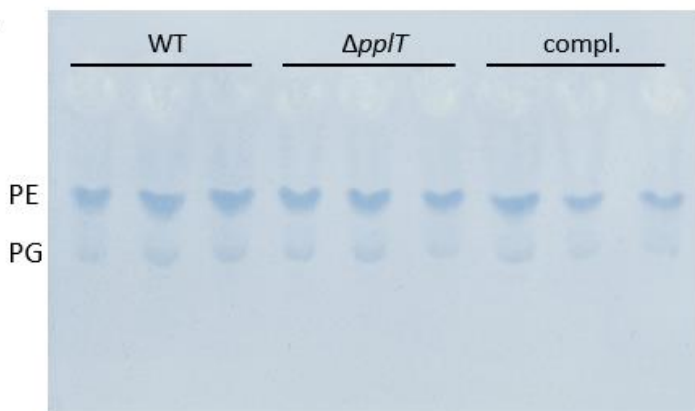


Figure 3: Genetic context and interaction partners of PpIT in *E. coli*. (A) PpIT is encoded in an operon together with YbhP, a protein of unknown function, and the cardiolipin synthase ClsB in Enterobacteriaceae, including the genera *Escherichia*, *Shigella*, *Klebsiella*, and *Pantoea*. The genes of the operon are not drawn to scale. (B) Schematic representation of the phospholipid synthesis pathways in *E. coli*. Cytidine diphosphate diacylglycerol (CDP-DAG), phosphatidylglycerol-3-phosphate (PGP), phosphatidylglycerol (PG), cardiolipin (CL), phosphatidylserine (PS), phosphatidylethanolamine (PE). Enzymes are marked in blue or grey, if they interacted with PpIT or not, respectively. (C) Interaction studies with PpIT and lipid-biosynthetic enzymes using the bacterial two-hybrid system and β -galactosidase assay for quantification. Data represent means plus SD of five biological replicates. Statistical significances were determined by two-way ANOVA followed by Dunnett's test in comparison to the negative control (ns, not significant; ****, $P < 0.0001$). Figures A and B were created with BioRender.com.

A



B

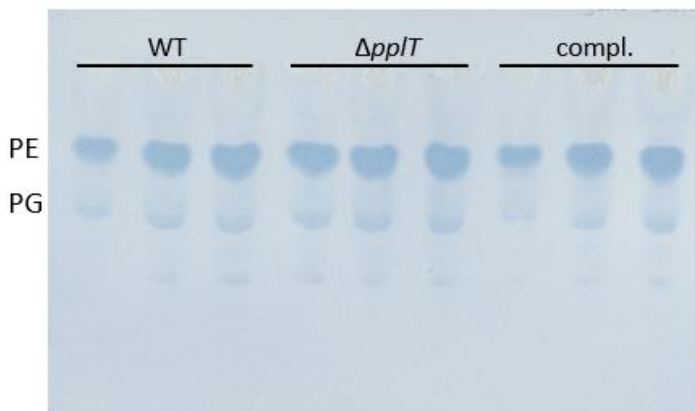


Figure 4: Impact of PplT on cell membrane lipid pattern. Detection of phospholipids of *E. coli* CFT073 WT, *pplT* mutant and complemented mutant at exponential (A) or stationary (B) growth phase. Total lipids were isolated, separated via thin-layer chromatography and stained using molybdenum blue spray reagent. PE and PG spots are indicated, concentrations of the minor lipids PS and CL are too low to be detectable. Three biological replicates are represented.

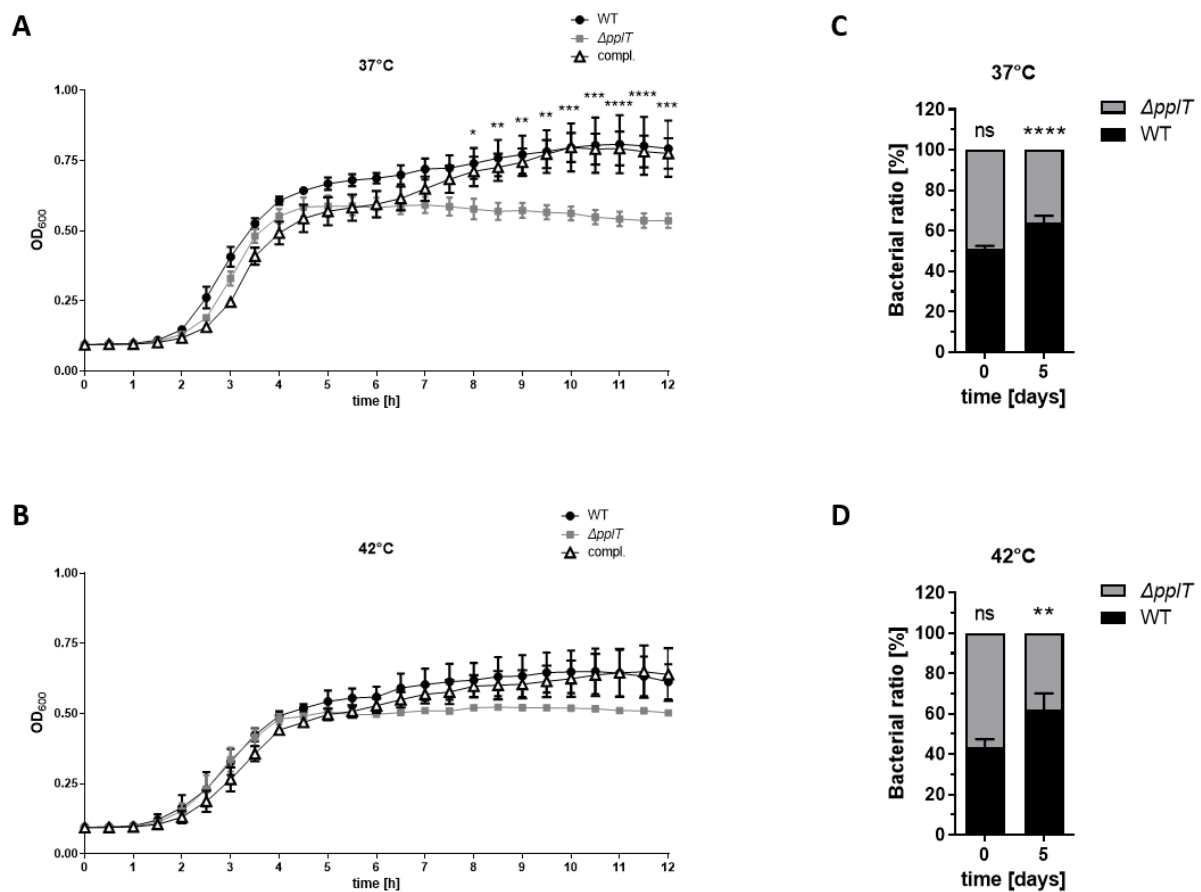


Figure 5: The *E. coli* *ppIT* mutant exhibits a growth deficit compared to the WT. Growth curves of *E. coli* CFT073 WT, *ppIT* mutant and complemented mutant at 37°C (A) or 42°C (B). Means of three biological replicates plus SEM are shown. The difference in growth between WT and *ppIT* mutant was statistically analyzed by two-way ANOVA (*, P < 0.05; **, P < 0.01; ***, P < 0.0005; ****, P < 0.0001). Competition assay of WT and the *ppIT* mutant over five days at 37°C (C) or 42°C (D). Means of three biological replicates with SD are shown. Data were statistically analyzed by two-way ANOVA and compared to the WT at the appropriate timepoint (ns, not significant; **, P < 0.01; ****, P < 0.0001).

Supporting Information

Table S1: Bacterial strains.

Strain	Characteristics
<i>E. coli</i> CFT073	Uropathogenic wild type strain [31]
<i>E. coli</i> CFT073 <i>ΔpplT</i>	<i>pplT</i> chromosomal deletion mutant, <i>pplT</i> gene was replaced by kanamycin resistance cassette, Kan ^R . This study.
<i>E. coli</i> CFT073 <i>ΔpplT</i> pRB <i>pplT</i>	<i>pplT</i> deletion mutant complemented by plasmid-encoded <i>pplT</i> version. This study.

Table S2: Plasmids.

Plasmid	Characteristics
pRB474 <i>pplT</i>	<i>pplT</i> gene cloned in <i>E. coli</i> / <i>S. aureus</i> shuttle vector pRB474 [33], Amp ^R .
pKD13	Template for Kanamycin resistance cassette. Amp ^R , Kan ^R [32].
pKD46	Lambda Red helper plasmid, Lambda Red expression inducible by L-arabinose. Amp ^R [32].
pKT25- <i>clsA</i>	<i>clsA</i> gene encoded on low copy number plasmid pKT25 (Euromedex), fused to the C-terminal end of the adenylate cyclase fragment T25. This study.
pKT25- <i>clsB</i>	<i>clsB</i> gene encoded on low copy number plasmid pKT25 (Euromedex), fused to the C-terminal end of the adenylate cyclase fragment T25. This study.
pKT25- <i>clsC</i>	<i>clsC</i> gene encoded on low copy number plasmid pKT25 (Euromedex), fused to the C-terminal end of the adenylate cyclase fragment T25. This study.
pKT25- <i>ybhP</i>	<i>ybhP</i> gene encoded on low copy number plasmid pKT25 (Euromedex), fused to the C-terminal end of the adenylate cyclase fragment T25. This study.
pKT25- <i>pssA</i>	<i>pssA</i> gene encoded on low copy number plasmid pKT25 (Euromedex), fused to the C-terminal end of the adenylate cyclase fragment T25. This study.
pKT25- <i>psd</i>	<i>psd</i> gene encoded on low copy number plasmid pKT25 (Euromedex), fused to the C-terminal end of the adenylate cyclase fragment T25. This study.
pKT25- <i>pgsA</i>	<i>pgsA</i> gene encoded on low copy number plasmid pKT25 (Euromedex), fused to the C-terminal end of the adenylate cyclase fragment T25. This study.
pKT25- <i>pgpA</i>	<i>pgpA</i> gene encoded on low copy number plasmid pKT25 (Euromedex), fused to the C-terminal end of the adenylate cyclase fragment T25. This study.
pKT25- <i>pgpB</i>	<i>pgpB</i> gene encoded on low copy number plasmid pKT25 (Euromedex), fused to the C-terminal end of the adenylate cyclase fragment T25. This study.
pKT25- <i>pgpC</i>	<i>pgpC</i> gene encoded on low copy number plasmid pKT25 (Euromedex), fused to the C-terminal end of the adenylate cyclase fragment T25. This study.
pKT25- <i>zip</i>	Leucine zipper of GCN4 fused to the C-terminal end of the adenylate cyclase fragment T25. BATCH system kit, Euromedex.
pUT18C- <i>pplT</i>	<i>pplT</i> gene encoded on high copy number plasmid pUT18C (Euromedex), fused to the C-terminal end of the adenylate cyclase fragment T18. This study.
pUT18C- <i>zip</i>	Leucine zipper of GCN4 fused to the C-terminal end of the adenylate cyclase fragment T18. BATCH system kit, Euromedex.

Table S3: Primers.

Primer	Sequence 5' → 3'	Usage
<i>pplT_KO_5</i>	ATGCACATACTAAAGAACCTAACTATACTT	

	CACATGCCGCTTCATTTTTGTAGGCTGG AGCTGCTTCG	Amplification of kanamycin resistance cassette from pKD13 with overhang homolog to the chromosomal <i>ppIT</i> surrounding; for construction of the chromosomal <i>ppIT</i> deletion mutant in <i>E. coli</i> CFT073.
ppIT_KO_6	GAAACGCAGGATCGGGTAGAAACTGAAA ACACGGGGTAAACCCCTGATGATTCCGG GGATCCGTCGACC	
pKD46_gone_1	CCCGTGCCTTGATGACGATG	Primers to confirm the curing of the helper plasmid pKD46.
pKD46_gone_2	GGATTCAATTGCTCTGCTCAAAGTCC	
pRB_ppIT_BamHI_fw	AAATTATggatccCAGAGGAGGTCGGCTGA TGAGTAAATCAC	Cloning of <i>ppIT</i> into pRB474 for plasmid-based complementation of the <i>ppIT</i> deletion mutant.
pRB_ppIT_EcoRI_rev	AAATTATgaattcAACTAAACTTCACATGCC GCTTC	
ppIT_up	ggttcggtgtgtttatagg	Sequencing primers to verify the chromosomal ppIT deletion mutant.
ppIT_down	cttcccccgcgtgg	
clsA_BamHI_for	TAATCggatccTATGACAACCGTTATACG	Cloning of <i>clsA</i> from <i>E. coli</i> CFT073 into pKT25 for bacteria two-hybrid.
clsA_EcoRI_rev	ACGTTgaattcTTACAGCAACGGGCTG	
clsB_BamHI_for	TCATTggatccTATGAAATGTAGCTGGCGCG	Cloning of <i>clsB</i> from <i>E. coli</i> CFT073 into pKT25 for bacteria two-hybrid.
clsB_EcoRI_rev	ACTCAGaattcTCAGGGTTTACCCCCGTG	
clsC_BamHI_for	GTCTGTggatccTATGATGAAGAAAACGCCAC	Cloning of <i>clsC</i> from <i>E. coli</i> CFT073 into pKT25 for bacteria two-hybrid.
clsC_EcoRI_rev	CGCGTgaattcTTACAATAACCATTCCACGG	
ybhP_BamHI_for	GAAAATggatccTATGCCGATCAAACAC	Cloning of <i>ybhP</i> from <i>E. coli</i> CFT073 into pKT25 for bacteria two-hybrid.
ybhP_EcoRI_rev	ACATTgaattcTCATAAATGAATCTCCGC	
pssA_BamHI_for	CATCCggatccTATGAAAATGACAAAACCTGG	Cloning of <i>pssA</i> from <i>E. coli</i> CFT073 into pKT25 for bacteria two-hybrid.
pssA_EcoRI_rev	CAGGGGaaattcTTACTGCGTGGTACCG	
psd_BamHI_for	CACTGTggatccGATGTTGTCAAAATTAAAGCG	Cloning of <i>psd</i> from <i>E. coli</i> CFT073 into pKT25 for bacteria two-hybrid.
psd_KpnI_rev	TGTGAGaattcTTACAGGATGCGGCTAATTAAATC	
pgsA_BamHI_for	GCTACggatccCTGTTAAATTCTTTAAAC	Cloning of <i>pgsA</i> from <i>E. coli</i> CFT073 into pKT25 for bacteria two-hybrid.
pgsA_EcoRI_rev	ATGGAggtaccTTAGACCTGGTCTTTTTG	
pgpA_BamHI_for	GTCATggatccTATGCAATTAAATATCCCTAC	Cloning of <i>pgpA</i> from <i>E. coli</i> CFT073 into pKT25 for bacteria two-hybrid.
pgpA_EcoRI_rev	AACCGAgaattcTCACTGATCAAGCAAATCTG	
pgpB_BamHI_for	AAGGAggatccTATGACCATTGCCACGCC	Cloning of <i>pgpB</i> from <i>E. coli</i> CFT073 into pKT25 for bacteria two-hybrid.
pgpB_EcoRI_rev	CACAAgaattcCTACGACAGAAATACCCAGC	
pgpC_BamHI_for	GAGGCggatccCATGCGTTCGATTGCC	Cloning of <i>pgpC</i> from <i>E. coli</i> CFT073 into pKT25 for bacteria two-hybrid.
pgpC_EcoRI_rev	CAGCGgaattcTTAACTTCTGTTCTCGTTG	
pUT18_PpIT_BamHI_for	CCCTGggatccGATGAGTAAATCACACCCGCG	Cloning of <i>ppIT</i> from <i>E. coli</i> CFT073 into pUT18C for bacteria two-hybrid.
PpIT_EcoRI_rev	ATACTgaattcTCACATGCCGCTTCATTTC	
pKT25 fw_2	CAACTCCGCGACTCGGCG	Sequencing primer to verify insert of pKT25.
pKT25 rev	gattaagtggtaacgcag	
pUT18C for	CGTCACCCGGATTGCGGC	Sequencing primer to verify insert of pUT18C.
pUT18C rev	cggggctggcttaactatgc	

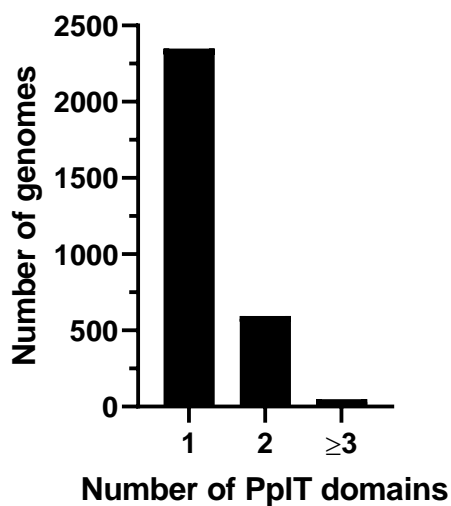


Figure S1: Most PpIT containing genomes of prokaryotes harbor only one homolog. Number of genomes with one, two or more genes encoding PpIT domains are shown.